

Electrodynamic processes in a spiral MHD pump of transformer type

© S.Yu. Khripchenko, E.Yu. Tonkov

Institute of Continuous Media Mechanics, Ural Branch, Russian Academy of Sciences,
614013 Perm, Russia

e-mail: khripch@icmm.ru, tonkoveu@mail.ru

Received May 16, 2024

Revised July 7, 2024

Accepted July 7, 2024

The creation of nuclear power plants using lead as a coolant makes it relevant to study and design devices capable of effectively pumping it. The purpose of this study is to evaluate the efficiency of the pressure developed in the stop mode by a spiral-MHD pump of a transformer type, capable of creating high pressures even when working with low-conductivity liquid metals. The paper presents a numerical simulation of electrodynamic processes in such a pump. The paper presents an estimated analytical dependence that helps to compare the characteristics of various versions of the designed pump without calculation packages. As part of the verification of the mathematical model, the experimentally studied design was calculated using the estimated form and numerical model. The paper presents the pump characteristics in the stop mode for some of its design options, as well as when it works with metals of different electrical conductivities. A comparison of calculations using the estimated formula and the numerical model with the experimental results was made. It is shown that the pump can create high pressures of the order of units of megapascals, working even with metals such as liquid lead, which has low electrical conductivity.

Keywords: MHD pump, magnetic hydrodynamics, numerical modeling, COMSOL Multiphysics, liquid lead.

DOI: 10.61011/TP.2024.10.59367.181-24

Introduction

Magnetohydrodynamic (MHD) pumps are used for pumping liquid metal in metallurgy and the nuclear industry. Electromagnetic forces acting on metal in the channels of such pumps and enabling their operation are the result of interaction of electrical current in the channel with a magnetic field. Depending on the method of electrical current generation in the channel, MHD pumps are divided into two categories: induction and conduction ones [1,2]. In induction pumps, electrical current in the channel is generated by an alternating magnetic field and interacts with it. In conduction pumps, current is supplied via electrodes and interacts either with a magnetic field from an external source or with its self-magnetic field. Since the electrical current generated by an external source in conduction pumps may reach a significant magnitude and may be supplied to a small-sized channel, pumps of this type are relatively compact and have the capacity to develop substantial pressure. It is worth noting that induction pumps are rather large. This is due to the fact that current in the channel of such pumps is induced by an external alternating magnetic field, and the channel dimensions needed to produce the necessary force are larger than the corresponding dimensions for conduction pumps. At the same time, induction pumps do not require separate power sources to produce a magnetic field and electrical current in the channel, and their efficiency normally exceeds the efficiency of conduction pumps. Transformer-type pumps, which combine the features of induction and conduction ones, are also available. In such pumps, electrical current supplied by

solid or liquid electrodes to the channel is induced according to the principle of a secondary turn of a transformer by the same alternating field with which it interacts in the channel of a pump, ensuring its operation [3–5].

An example here is a pump with a straight channel and a horseshoe-shaped busbar on both of its sides [3].

Electrical current in the busbar and the channel (as a secondary turn of a transformer) is induced by an alternating magnetic field produced by a special core. The path of this current through the channel is completed via the horseshoe-shaped busbar. Thus, current flows in one direction from one wall, which is in contact with one side of the horseshoe-shaped busbar, to the opposite wall, which is in contact with the other side. Electrical current in the channel interacts with the magnetic field that induced it, generating a volumetric electromagnetic force in liquid metal directed towards the horseshoe enveloping the channel. These forces govern the pump operation. This device was characterized and studied experimentally in [3]. It is similar both to a transformer (in terms of the current excitation method) and to a conduction pump (in terms of the method of supplying current to the channel), providing a combination of small size and the capacity to operate without a bulky separate power source.

The pump examined in the present study has a similar operating principle [5], but its channel *1* is twisted into a spiral to raise the developed pressure (Fig. 1), and its opposite sides *2* are positioned between poles *3* of magnetic circuit *4* of the magnetic system that produces an alternating magnetic field with magnetization coils *5*. Laminated ferromagnetic core *6* is inside the spiral between the poles.

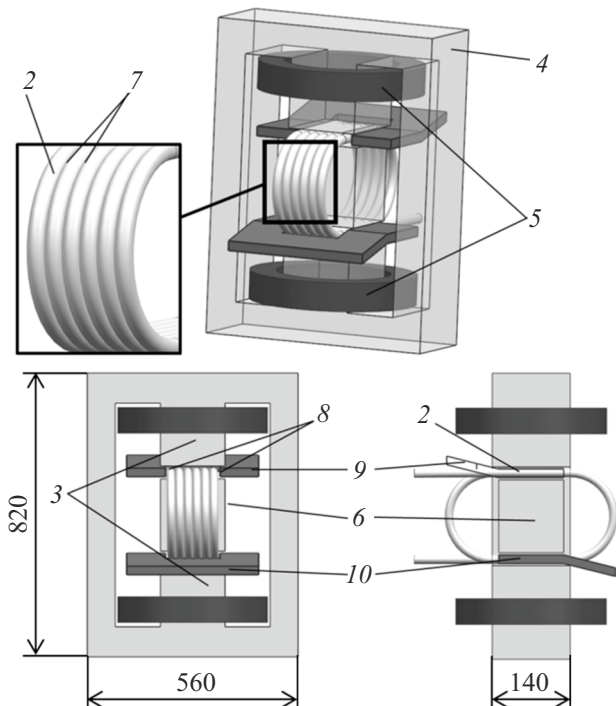


Figure 1. Spiral transformer MHD pump: 1 — spiral channel, 2 — side wall of the spiral channel, 3 — magnetic poles, 4 — magnetic circuit, 5 — magnetization coils, 6 — laminated ferromagnetic core, 7 — soldering points of tubes of the spiral channel, 8 — outer side walls of the spiral channel in contact with horseshoe-shaped busbars, and 9, 10 — horseshoe-shaped closing busbars. The distribution of magnetic field lines in the magnetic circuit is shown on the right.

Side walls 7 of adjacent turns of the spiral channel, which are positioned between the poles of magnetic circuit 4, are in good electrical contact, which is established by welding or soldering. The outer walls of the outermost turns of the spiral on two opposite lateral sides are in contact 8 with the longitudinal parts of two horseshoe-shaped busbars 9, 10, which „envelop“ the first and second poles of the magnetic system from opposite sides. A distinguishing feature of this device is that the channels do not lie in one plane in the same pole gap of the magnetic circuit; instead, they are combined into a single spiral with its two opposite sides positioned in two pole gaps of the magnetic circuit. Regardless of the number of turns of the spiral channel, the pump has only two horseshoe-shaped busbars that are connected by their longitudinal parts to the outermost turns of the channel and envelop the poles of the magnetic circuit from opposite sides.

The device under study is similar in its operating principle to the MHD pump discussed in [3]. Just as in [3], the magnetic field in tubes of the channel and busbars induces electrical current that flows across these tubes (Fig. 2), which are located in the gaps between poles 3 and laminated core 6 (Fig. 1), through the corresponding horseshoe-shaped busbars 1 (Fig. 2). The electrical current

in tubes 2 (Fig. 2) interacts with the magnetic field in the gaps and produces a volumetric force acting on liquid metal in the tubes, enabling operation of the pump. Since all the tubes in the spiral channel are connected in series, the pressures developed in them are combined.

1. Determination of the pressure developed by the pump

Figure 2 shows the schematic diagram of a part of spiral channel 2, which is located between the poles of the core, with horseshoe-shaped closing busbar 1 and their equivalent electrical circuit 4. The designations are as follows: channel tube diameter — a ; tube wall thickness — d_w ; height of the soldered joint between the channel tubes — δ ; length of the horseshoe-shaped busbar segment soldered to the channel — l ; electrical resistance of the horseshoe-shaped closing busbar — R_b ; and electrical resistance of the spiral channel in the region of the core poles — R_{ch} .

2. Analytical evaluation of the pressure developed by the pump

To estimate the pressure developed by such a pump, one may render the region of the spiral channel in which the turns are soldered together as a single rectangular region 0, A, B, l with liquid metal conductivity σ_{liq} (Fig. 2). The length of side 0, l of this region is l , while the length of side 0, A is aN , where a is the width of one turn of the channel, and N is the number of turns. Let us assume that region 0, A, B, l is in a uniform alternating magnetic field with frequency f and magnetic induction vector B normal to the plane of this region; the magnetic field outside of it is zero. The region is encircled by electrically conducting busbar 1 (Fig. 2), which is in electrical contact with sides 0, l and A, B. The conductivity of the busbar may be considered infinite. The magnetic flux in circuit 3 (Fig. 2), which encircles a part of the region under consideration and a part of the conducting busbar, is then written as

$$\Phi = BxaN. \quad (1)$$

If the magnetic field varies with time according to a harmonic law with circular frequency $\omega = 2\pi f$, one may obtain an estimate of e.m.f. generated in the considered circuit from Faraday's law:

$$EMF = -\omega BxaN. \quad (2)$$

If the electrical field in the region under consideration is, in common with the magnetic field, uniform,

$$EMF = E_y aN. \quad (3)$$

Using Ohm's differential law $j_y = \sigma_{liq} E_y$ and expressions (1)–(3), we find an estimate for the current density in the region under consideration:

$$J_y = EMF \frac{\sigma_{liq}}{aN} = \omega Bx\omega_{liq}. \quad (4)$$

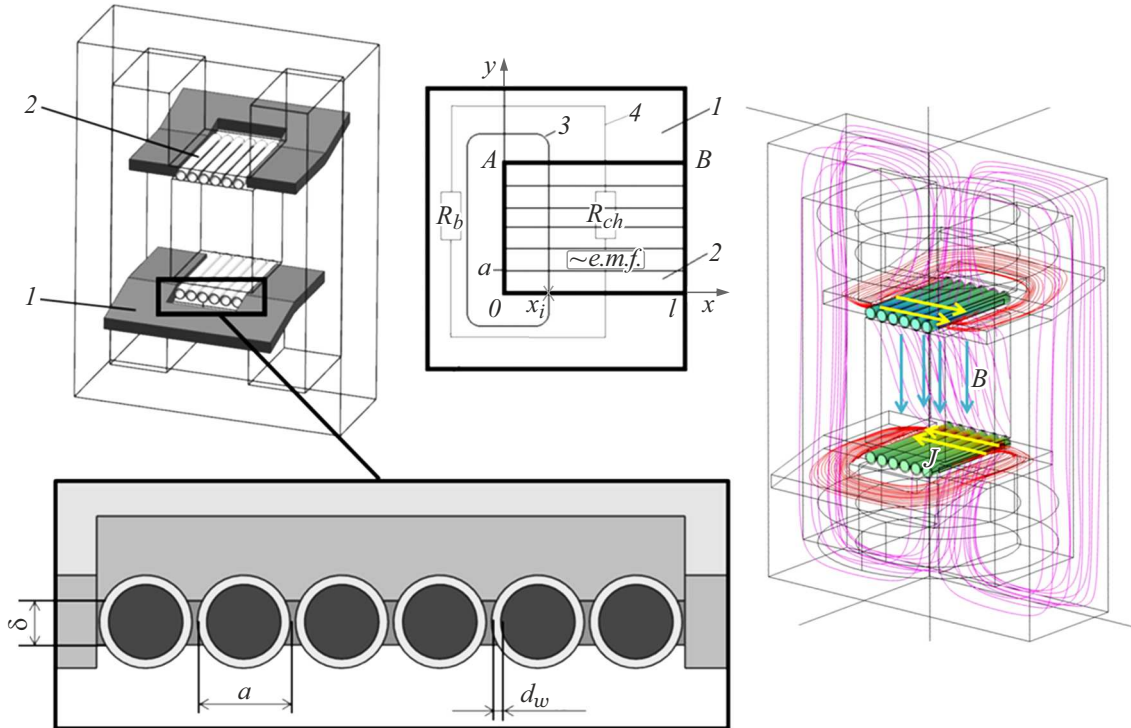


Figure 2. Schematic diagram of a simplified model of the considered pump: 1 — horseshoe-shaped closing busbar, 2 — tubes of the spiral channel with a diameter of a and a wall thickness of d_w that are positioned in the pole gap of the magnetic circuit and soldered together with solder with a height of δ , 3 — imaginary circuit encircling the magnetic flux in the pole gap, and 4 — equivalent electrical circuit. The distribution of electrical current lines in tubes of the channel and horseshoe-shaped busbars is shown on the right.

The volumetric electromagnetic force may then be estimated as

$$f_x = j_y B = \omega B^2 x \sigma_{\text{liq}}. \quad (5)$$

Integrating expression (5) along axis x from 0 to l , one may obtain an expression for estimating the electromagnetic pressure produced by region 0, A, B, l :

$$\Delta p = \int_0^l f_x dx = \frac{\omega \sigma_{\text{liq}} B^2 l^2 K_\phi \gamma}{2}. \quad (6)$$

The examined region consists of N segments (with width a and length l), which are parts of the turns of the spiral channel. The same pressure (6) is produced in each segment. Since the segments of the spiral channel are connected hydraulically in series and the examined pump features two regions with horseshoe-shaped busbars, the resulting pressure produced by the spiral channel is $2N$ times higher than pressure (6) developed in a single segment:

$$\Delta p = 2N \int_0^l f_x dx = N \omega \sigma_{\text{liq}} B^2 l^2 K_\phi \gamma \xi. \quad (7)$$

To obtain a more accurate result, one needs to multiply expression (7) by attenuation coefficient K_ϕ , which is related to the phase shift between the magnetic field and the current induced by it in the channel, and by coefficient γ , which is

needed to take the finite nature of conductivity of the closing busbar into account.

Relying on the results obtained in [4], we may set $K_\phi = 0.42$. Coefficient γ may be determined by presenting the channel and the horseshoe-shaped busbar as equivalent electrical circuit 4 (Fig. 2).

Coefficient $\gamma = R_{ch}/(R_{ch} + R_b)$, where R_{ch} is the electrical resistance of region 0, A, B, l , R_b is the resistance of the horseshoe-shaped busbar, and e.m.f. (Fig. 2) is the electromotive force induced by the alternating magnetic field. One should also take into account the fact that the electrical current induced in the channel is distributed between liquid metal and its conductive walls. Thus, the electrical current in liquid metal is slightly weaker than the total induced current. To take this effect into account, attenuation coefficient ξ , which is lower than unity and depends on the conductivity of liquid metal and the channel walls and the geometry of the channel, is introduced into expression (7). Coefficient ξ may be written as

$$\xi = \frac{\sigma_{\text{liq}} \Delta}{(\sigma_{\text{liq}} \Delta + \sigma_w d_w)}, \quad (8)$$

where Δ , d_w , and σ_w are the thickness of the liquid metal layer in the channel, the thickness of the wall, and its conductivity, respectively.

If liquid metal moves within the channel under the influence of electromagnetic forces, an electrical field is

produced in the process of its motion within an alternating magnetic field. This electrical field directed opposite to the one induced by the alternating magnetic field. To take this phenomenon into account, one may introduce product νB with the proper sign into expression (3).

The resulting expression for estimating the magnitude of electromagnetic pressure developed by the pump when liquid metal moves through its channel is

$$\Delta p = \xi \gamma N B^2 \sigma_{\text{liq}} (\omega l^2 K_\varphi - \nu l) - k \frac{N \rho \nu^2}{2}. \quad (9)$$

Term $k N \rho \nu^2 / 2$, which is needed to take into account the hydraulic resistance of the channel, was introduced into (9) [6].

In the present study, the results obtained using expression (9) were compared with the experimental data from [4]. The pump examined in [4] is similar to the one studied here with a spiral channel with 0.5 turns. Gallium was the liquid medium. Thus, based on the published data, $K_\varphi = 0.42$ and $B = 0.38$ T. In the conditions of [3], one may set $\gamma \approx 0.59$.

In the stop mode, expression (9) yields a pressure of $4.14 \cdot 10^5$ Pa developed by the pump. The experimentally obtained pressure in [3] was 15% ($3.5 \cdot 10^5$ Pa) lower than the one calculated using formula (9). The discrepancy between estimates and the experimental data may be attributed to the fact that the so-called armature reaction, which reduces the pressure developed by the pump, and the contact resistance in current flow through the channel walls were neglected in calculations. In addition, certain design parameters were not specified in the cited paper, and their approximate values were used.

Expression (9) is by no means highly accurate, but may be used to obtain preliminary estimates and compare various options in the process of engineering design of pumps of this kind.

3. Numerical calculation

The performance parameters of the pump under consideration were calculated numerically and compared with the results obtained using the evaluation formula. Only the electrodynamic part of the general problem (without the flow of liquid metal within the channel) was modeled. In non-magnetic gaps of the core where the spiral is located, the turns of the channel are soldered together at their sides and are in electrical contact with each other; there is no electrical contact in the region outside the gaps. In view of this, electrical current in the channel is induced by an alternating magnetic field only in the region of the gaps. Therefore, the problem may be simplified, and only the channel segments located in the non-magnetic gaps (Fig. 2) may be considered instead of the entire spiral channel.

The following equations characterize the electromagnetic processes in the core and the channel in the low-frequency approximation without regard to the motion of liquid

metal [7–10]:

$$\begin{cases} \mathbf{E} = -i\omega\mathbf{A} \\ \nabla \times \mathbf{H} = \mathbf{J} \\ \mathbf{B} = \nabla \times \mathbf{A} \\ \mathbf{J} = \sigma \mathbf{E} + i\omega \varepsilon_0 \varepsilon_r \mathbf{E} \\ \text{div} \mathbf{B} = 0 \end{cases}, \quad (10)$$

where \mathbf{A} is the vector potential, \mathbf{H} is the magnetic field vector, \mathbf{J} is the current density vector, \mathbf{B} is the magnetic induction vector of the field, \mathbf{E} is the electrical field vector, ε_r is the relative permittivity of the material, ε_0 is the vacuum permittivity, and i is an imaginary unit.

It was assumed that the magnetic field produced by alternating current in the magnetization coils of the pump varies with time in accordance with a harmonic law [11]. A homogenized model [12] for the analysis of coils, which have the shape of a cylinder with a cross-sectional area approximately equal to the cross-sectional area of wound wires, was adopted. The electrical current density in the coils was determined as [12]

$$\mathbf{J}_e = \frac{N I_{\text{coil}}}{A} \mathbf{e}_{\text{coil}}, \quad (11)$$

where N is the number of coil turns, I_{coil} is the amplitude of current in the coils, A is the cross-sectional area of the coil, and \mathbf{e}_{coil} is the vector indicating the direction of current flow in the coil.

Hysteresis and Joule losses in the core were not taken into account in the analysis of the magnetic system; it was also assumed that the core is made of transformer steel and its magnetic permeability is independent of the magnetic field.

The condition of magnetic field vanishing at infinity was modeled by choosing a sufficiently large computational domain that included the entire object under study. Its geometric dimensions were specified in such a way that the domain size did not affect the calculated electrodynamic parameters of the object.

It was assumed that electrical current does not flow through the channel walls and penetrate through the outer boundaries of the horseshoe-shaped busbars. The condition of „magnetic insulation“ [10] was satisfied for the vector potential of the magnetic field at the boundary of the computational domain:

$$\mathbf{n} \times \mathbf{A} = 0, \quad (12)$$

where \mathbf{n} is the surface normal of the computational domain boundary.

In the present study, a quasi-static process [13] of pump operation was modeled, wherein the pressure produced in the stop mode was determined without regard to hydrodynamic processes. The module of frequency analysis of electromagnetic processes from the COMSOL Multiphysics package was used for the electrodynamic calculation.

To assess the reliability of the mathematical model used, a numerical experiment with a pump design similar to the one from [3] was carried out. In tests with gallium [3]

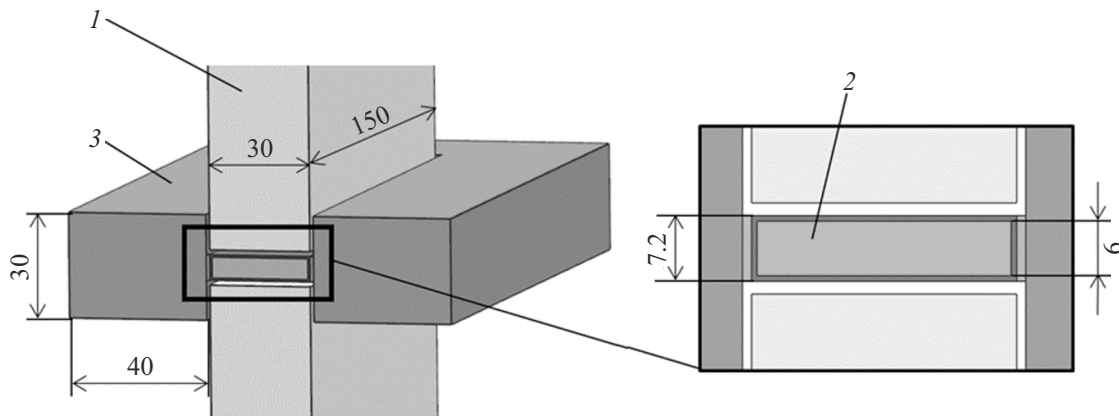


Figure 3. Reconstructed configuration of the channel and the magnetic system of the pump from [3]: 1 — magnetic system poles, 2 — pump channel, 3 — horseshoe-shaped closing copper busbar.

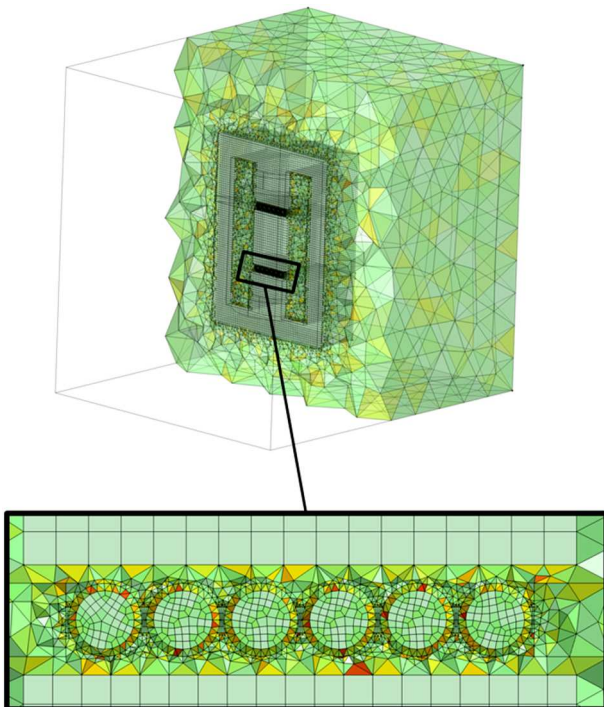


Figure 4. Grid model of the pump core and the turns of the spiral channel located in the pole gap.

and an effective magnetic field induction of 0.38 T, the pump produced a pressure of 0.35 MPa at $\cos \varphi = 0.42$. The geometry of the pump examined experimentally in [3] (Fig. 3) was used in the numerical model.

The authors of [3] did not provide a diagram of the pump (only a worded description is available), and certain dimensions and parameters of the magnetization coil were not specified. The calculated pressure developed by a pump with such parameters was 0.41 MPa, and $\cos \varphi = 0.7$. The obtained values differ from the experimental data. The calculated pressure is 15% higher than the one reported in [3], which is attributable to the assumed constancy

of magnetic permeability of the core; the fact that the conductivity values of the walls and liquid gallium at the temperature of the experiment were not provided in the cited paper; and the lack of description of certain structural elements, parameters of the magnetization coils, and the size of the non-magnetic gap. However, the results of our calculations of the developed pressure are close to the experimental data, suggesting that the mathematical model is applicable. They are also close to the results of calculations by evaluation formula (8).

At the next stage of the study, its main object (transformer-type pump [5]; see Fig. 1) was modeled numerically. The spiral channel of this pump features six turns of a stainless steel tube (12Kh18N10T) with a diameter of 20 mm and a wall thickness of 2 mm. The channel is positioned in two pole gaps 30 mm in height of an O-shaped core, which produces an alternating magnetic field in these gaps. The pole size is 150×120 mm. The turns of the spiral channel located in non-magnetic gaps are soldered together with silver solder at their side walls. Two horseshoe-shaped copper busbars are soldered to the outermost turns of the channel located in the core gaps (Fig. 1). The alternating magnetic field produced by the magnetic system of the pump in the gaps induces an e.m.f. in the sections of the spiral channel located in these gaps. This e.m.f. closes through the horseshoe-shaped busbars enveloping the poles of the core on both sides and generates electrical current in the channel. The interaction of this current and the magnetic field inducing it generates volumetric electromagnetic forces that produce pressure in each turn of the spiral channel; since all sections of the spiral channel tube where these forces act are hydraulically connected in series, the resulting pressure is amplified by a multiple of the doubled number of turns of the spiral channel.

A grid model with 1.19 million elements was adopted in numerical modeling of the object under consideration. The dimensions and the number of elements in the entire computational domain were chosen so as to provide fine

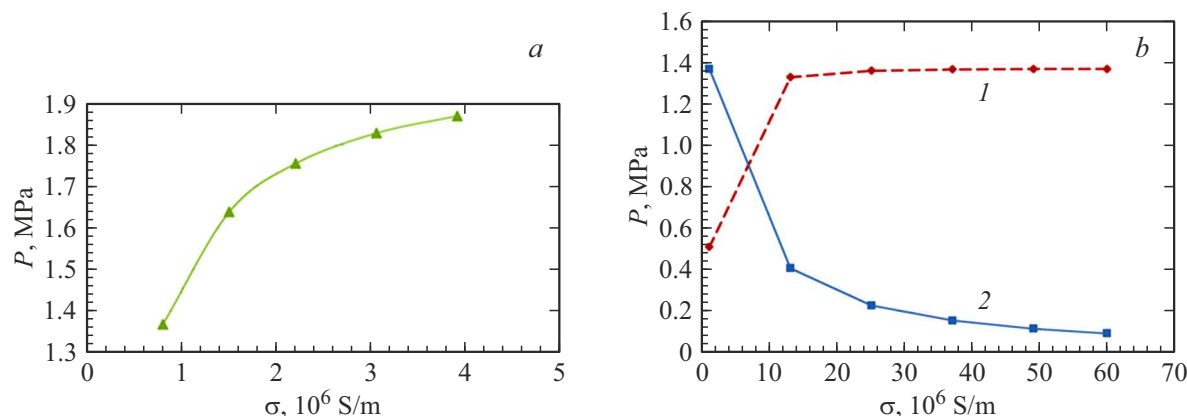


Figure 5. *a* — pressure developed by the pump vs. conductivity of the pumped liquid metal, *b* — pressure developed by pump vs. conductivity of closing bus — 1 and vs. conductivity of walls of pump channel — 2.

discretization of the walls of the examined channel consisting of tubes with a diameter of 20 mm and a thickness of 2 mm (Fig. 4). In the calculation model, the electrical contact between the tubes and the horseshoe-shaped busbar is established by special solder that connects electrically the tube turns to each other. It is represented as a separate domain with its own material properties and dimensions in the region of the pole gaps.

4. Results of the numerical experiment

The numerical experiment revealed that the examined pump [5] with a spiral channel featuring six turns (Fig. 1) develops a pressure of 1.37 MPa (Fig. 5) in the stop mode with a coil rated at 29700 ampere-turns. An alternating electrical current with an amplitude up to 15266 A is induced in this case in the channel and in the closing horseshoe-shaped busbar. The corresponding amplitude value of current in liquid lead in the pump channel is 13293 A.

It was found in the numerical experiment (Fig. 5, *a*) that the pressure developed by the pump depends on the conductivity of pumped metal. The volumetric force gets stronger with conductivity of the pumped medium, although the increase in pressure becomes less pronounced as this conductivity increases. This is due to the fact that the ohmic resistance of the circuit (channel–closing busbar) decreases within increasing conductivity of liquid metal, thus raising the magnitude of induced current and, consequently, pressure developed by the pump. However, there is a limit to this process. Since the resistance of the circuit cannot be lower than the resistance of the closing busbar, the magnitude of induced current is also limited.

The pressure varies in much the same way when the conductivity of the closing busbars increases (Fig. 5, *b*, curve 1). When the ohmic resistance of the closing busbar decreases, the total resistance of the circuit cannot fall below the resistance of the channel, thus limiting the increase in induced current and, consequently, the rise

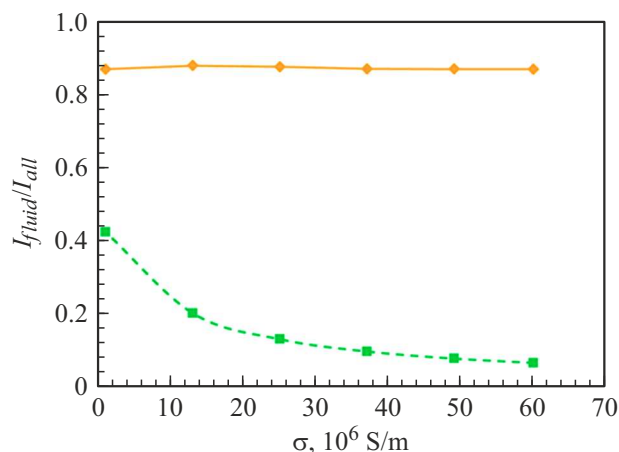


Figure 6. Dependences of the ratio of current flowing through the liquid to the total current on the conductivity of the channel walls (1) and on the conductivity of the horseshoe-shaped busbar (2). The liquid metal in the channel is lead.

of pressure developed by the pump. A different pattern is observed when the conductivity of the channel walls increases (Fig. 5, *b*, curve 2). Their shunting effect becomes more pronounced in this case, and the current in liquid metal grows weaker (Fig. 6, curve 1), which leads to a reduction in pressure. However, the total channel resistance decreases, and the total induced current grows stronger as a result. This is the reason why the observed reduction in current in liquid metal is not so sharp. Since the pressure developed by the pump depends linearly on current in liquid metal, the above considerations are also applicable to it.

The total current in the circuit and in liquid metal increases with an increase in conductivity of the horseshoe-shaped busbar. Its growth stops at the moment when a certain level of conductivity of the closing busbar is reached. The current in liquid metal behaves in the same way. Owing to shunting by the channel walls, it is somewhat lower than

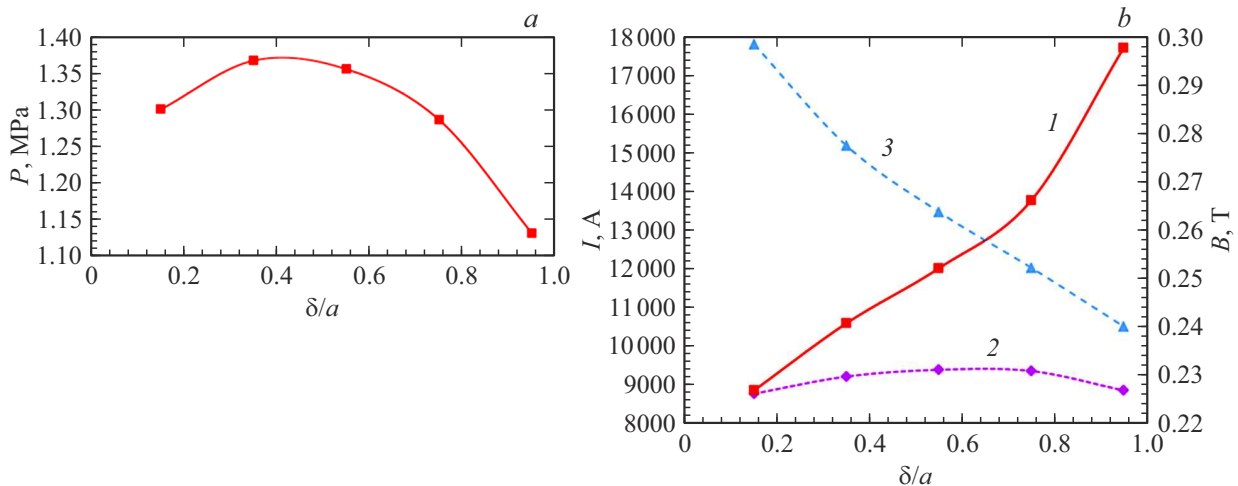


Figure 7. *a* — Dependence of the developed pressure on the ratio of the soldering height to the diameter of tubes (channel segments); *b* — dependences of the total induced current (curve 1); induced current in the liquid (curve 2); and magnetic field (curve 3) on the ratio of the soldering height to the tube diameter. The liquid metal in the channel is lead.

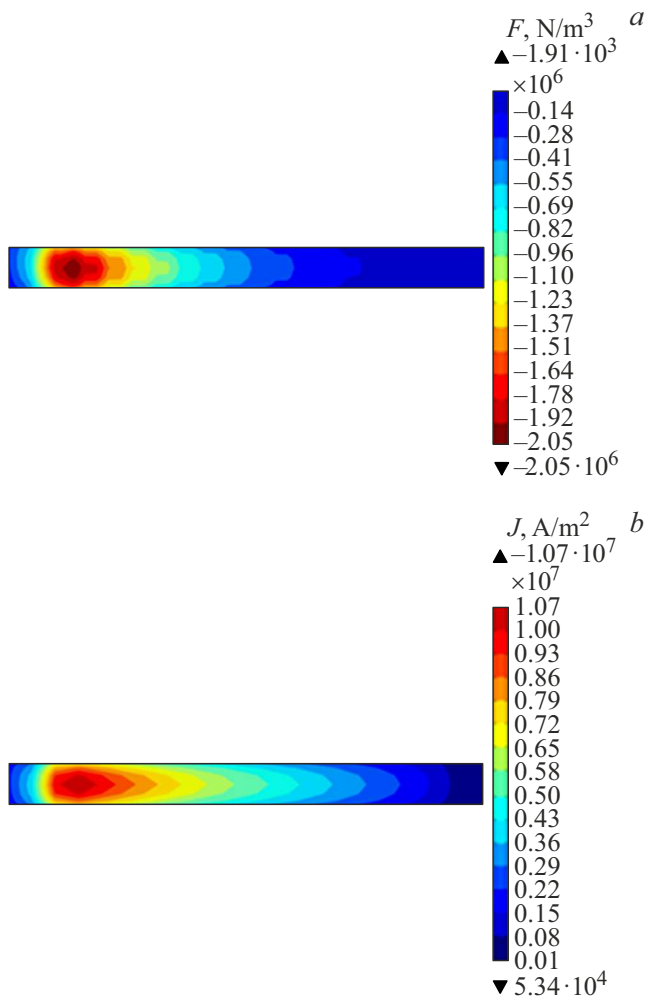


Figure 8. Distributions of volumetric force (*a*) and current density (*b*) along the length of a channel segment.

the total current of the circuit. At the same time, the ratio of these currents remains virtually constant (Fig. 6, curve 2).

When modeling the processes in the pump under consideration, we investigated the influence of soldering height δ (Fig. 2) on pressure developed by the pump (Fig. 7, *a*). The plot demonstrates that the developed pressure is maximized at a certain optimum soldering height. To study this dependence in detail, we analyzed the dependences of total current, current in liquid, and magnetic field (Fig. 7, *b*) on the relative soldering height. The best value of the ratio of the soldering height to the tube diameter (Fig. 7, *a*) is ~ 0.42 , while the maximum current in liquid (Fig. 7, *b*, curve 2) is achieved at a ratio of ~ 0.63 . This discrepancy is attributable to the fact that the total resistance of the circuit decreases with an increase in soldering height, which leads to an increase in total current (Fig. 7, *b*, curve 1) and weakening of the magnetic field (Fig. 7, *b*, curve 3) due to a more pronounced armature reaction. The above reasoning explains the discrepancy between the soldering height levels corresponding to the maximum pressure and to the maximum current in liquid. The presence of an extremum in the plot of the dependence of current in liquid on the ratio of the soldering height to the channel diameter (Fig. 7, *b*, curve 2) is attributable to the fact that the shunting effect of the channel walls becomes less pronounced as the soldering height decreases, which leads to an increase in current flowing through liquid metal. At the same time, a reduction in soldering height leads to an increase in total resistance of the circuit, which, in turn, reduces the total current (in particular, the current flowing through liquid metal).

Additional results of numerical modeling are presented below. Figure 8 shows the distributions of volumetric force and current density along the length of a channel segment.

The distribution of current density in a channel with walls at the optimum soldering height is presented in Fig. 9.

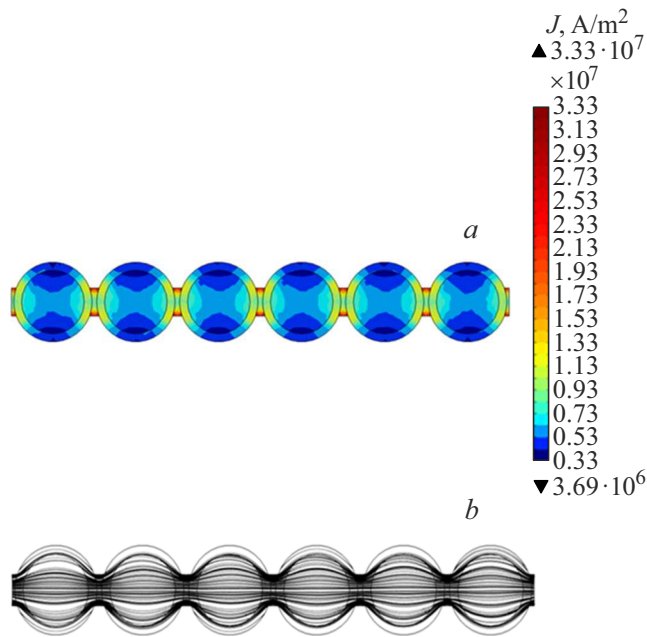


Figure 9. *a* — Distribution of current density over the walls of channel segments, liquid lead, and solder; *b* — electrical current density lines.

The shunting effect of the channel walls is evident. The current density lines are also shown, illustrating the current distribution between the channel and the walls.

A comparison was made between the pressure developed by a spiral pump with a channel of six turns (Fig. 1) calculated by an approximate formula and the pressure obtained via numerical modeling. A magnetic field of 0.3 T, a frequency of 50 Hz, six turns, $K_\phi = 0.66$ (obtained in the numerical model), $\gamma = 0.89$, and $\xi = 0.85$ were set in this formula. The pressure developed by a liquid-lead pump with conductivity $10^6 \Omega^{-1}\text{m}^{-1}$ is then 1.9 MPa, while numerical calculations yield 1.45 MPa. The difference is close to 24%.

Conclusion

The examined spiral transformer-type pump is compact and has the capacity to produce fairly high pressures (over 1 MPa) even when working with low-conductivity metals, such as liquid lead. In addition, it does not require special power sources and may be powered by industrial AC mains. The evaluation formula proposed above coupled with subsequent accurate numerical calculations may be used to explore various design options in the process of construction of pumps of this type with their parameters tailored to a specific production operation.

Funding

This study was carried out in accordance with fiscal plan No. 122030200191-9 of the Institute of Continuous Media Mechanics (Ural Branch, Russian Academy of Sciences).

Conflict of interest

The authors declare that they have no conflict of interest

References

- [1] A.I. Vol'dek. *Induktsionnye magnitogidrodinamicheskie mashiny s zhidkometallicheskim rabochim telom* (Energiya, L., 1970) (in Russian).
- [2] Yu.A. Birzvalk. *Osnovy teorii rascheta konduksionnykh nasosov postoyannogo toka* (Zinatne, Riga, 1968) (in Russian).
- [3] L.K. Brekson, N.I. Glazkov, V.D. Egorov, Yu.F. Merenkov, S.R. Troitskii *Eksperimental'noe issledovanie odnofaznogo MGD-Nasosa s elektromagnitnoi asimmetrii* (Devyatoe Rizhskoe soveshchanie po magnitnoi gidrodinamike, chast' II, tezisy dokladov, Riga, 1978), pp. 53–54 (in Russian).
- [4] Yu.F. Merenkov, I.V. Popkov. *Elektromagnitnyi nasos AS N 02N 4/20*. SU Patent No. 898575. Published on January 15, 1982. Byull. Izobret. No. 2 (in Russian).
- [5] S.Yu. Khripchenko, V.M. Dolgikh. *Elektromagnitnyi induktsionnyi nasos dlya zhidkikh provodyashchikh sred* (RF Patent No. 2810528, Application No. 2023119291) (in Russian).
- [6] I.E. Idel'chik. *Spravochnik po gidravlicheskim soprotivleniyam. 3-e izdanie, pererabotannoe i dopolnennoe* (Mashinostroenie, M., 1992) (in Russian).
- [7] C. Alberghi, L. Candido, R. Testoni, M. Utili, M. Zucchetti. *Energies*, **14** (17), 5413 (2021). DOI: 10.3390/en14175413
- [8] M. Zaja, A.A. Razi-Kazemi, D. Jovic. *High Voltage*, **5** (5), 549 (2019). DOI: 10.1049/hve.2019.0387
- [9] L.P. Aoki, H.E. Schulz, M.G. Maunsell. *An MHD Study of the Behavior of an Electrolyte Solution using 3D Numerical Simulation and Experimental results*. Excerpt from the Proceedings of 2013 COMSOL Conference in Boston, **15**, 65 (2013)
- [10] S.D. Samuilov, I.P. Shcherbakov, Y.N. Bocharov, S.I. Krivosheev, S.G. Magazinov. *Tech. Phys.*, **68** (8), 1108 (2023). DOI: 10.61011/TP.2023.08.57273.61-23
- [11] A.D. Podol'tsev, L.N. Kontorovich. *Tekh. Elektrodin.*, **6**, 3 (2011) (in Russian).
- [12] C.R. Vargas-Llanos, F. Huber, N. Riva, M. Zhang, F. Grilli. *Superconductor Sci. Technol.*, **35**, 41 (2022).
- [13] N.E. Jewell-Larsen, S.V. Karpov, I.A. Krichtafovitch, V. Jayanty, Ch.-P. Hsu, A.V. Mamishev. *ESA Annual Meeting on Electrostatics*, **1**, 20 (2008).

Translated by D.Safin